AIAA JOURNAL
Vol. 45, No. 5, May 2007

Technical Notes

TECHNICAL NOTES are short manuscripts describing new developments or important results of a preliminary nature. These Notes should not exceed 2500 words (where a figure or table counts as 200 words). Following informal review by the Editors, they may be published within a few months of the date of receipt. Style requirements are the same as for regular contributions (see inside back cover).

Nonlinear Aeroelastic Analysis of Control with Freeplay in Transonic Region

Young-Keun Park,* Jae-Han Yoo,* and In Lee†
Korea Advanced Institute of Science and Technology (KAIST), Daejeon 305-701, Republic of Korea

DOI: 10.2514/1.14068

Nomenclature

$[C]$	=	damping matrix
$\{F\}$	=	external aerodynamic force vector
$\{f(\alpha)\}$	=	restoring force vector due to structural nonlinear factor
$[GC]$	=	generalized damping matrix
$[GM]$	=	generalized mass matrix
$[GR]$	=	generalized restoring force vector defined as $[\phi_b]^T[K][\phi_b]\{q\} - [\phi_b]^T\{f(\alpha)\}$
$[K]$	=	linear stiffness matrix
K_α	=	linear stiffness at the freeplay node
M	=	Mach number
$[M]$	=	mass matrix
$\{Q\}$	=	generalized external aerodynamic force vector
$\{q\}$	=	generalized displacement vector
$\{R(u)\}$	=	restoring force vector including structural nonlinearities
S	=	wing area
s	=	freeplay angle at the freeplay node
U	=	freestream air velocity
$\{u\}$	=	displacement vector
α	=	pitch angle at the freeplay node
α_L	=	LCO amplitude of the pitch angle at the freeplay node
α_0	=	initial pitch angle at the freeplay node
ΔCp	=	pressure coefficient difference between the upper and the lower surfaces
ρ	=	freestream air density
$[\phi_b]$	=	modal matrix

Received 19 October 2004; revision received 28 November 2006; accepted for publication 15 January 2007.

*Graduate Research Assistant, Division of Aerospace Engineering, 373-1 Guseong-Dong, Yuseong-gu; currently with the Agency for Defense Development.

†Professor, Division of Aerospace Engineering, 373-1 Guseong-Dong, Yuseong-gu. Associate Fellow AIAA.

I. Introduction

DURING the past several decades, most aeroelastic investigations have been carried out under the assumption of linearity in aerodynamics and structures. However, a real air vehicle has structural nonlinearities such as freeplay, friction, and hysteresis. It also has aerodynamic nonlinearities caused by shock waves in the transonic region. In practice, these nonlinearities lead the limit cycle oscillation (LCO) and the transonic dip of air vehicle structures.

In particular, freeplay, one of the concentrated structural nonlinearities, is inevitable for control wings due to normal wear of components and manufacturing mismatches. It has been reported that the vibration of some aircraft in flight is closely related with freeplay [1]. According to the JSSG-2006 [2], the U.S. Department of Defense guidebook for air vehicle structural design, the freeplay of control surfaces should be limited for aeroelastic characteristics. The guidebook recommends the tightest freeplay for all-movable control wings, that is, less than 0.034 (peak to peak). As this guidance is very difficult to meet in practice, freeplay for all-movable control wings beyond the recommended limit is often justified based on test experience, such as flutter model tests, flight tests, etc., and to some extent on analyses.

Some aeroelastic analyses with freeplay have been performed in the past. Laurenson and Trn [3] used the describing function method to investigate the aeroelastic responses of a missile control surface with freeplay and showed that LCOs could be obtained at velocities below the linear flutter boundary. Kim and Lee [4] studied a 2-D flexible airfoil with freeplay, where the airfoil was modeled using beam elements. Bae and Lee [5] investigated the nonlinear aeroelastic characteristics of a wing with freeplay using frequency and time domain analyses. The frequency domain analyses were carried out by the describing function and the v-g methods. The time domain analyses were accomplished by time integration of the unsteady aerodynamic forces approximated by a rational function. However, most of these studies are restricted to a 2-D airfoil model and/or subsonic region. For aerodynamic nonlinearity, Kim and Lee [6] performed an aerodynamic analysis of a wing in the transonic region using the transonic small disturbance (TSD) code, which was also applied in the study. Kousen and Bendiksen [7] studied aeroelastic characteristics of 2-D airfoil models in the transonic region using the Euler equation and showed that LCOs could occur in the transonic region due to nonlinear aerodynamic forces induced by shock. They later extended the analysis to freeplay nonlinearity and showed the flutter velocity drops [8]. Kholodar and Dowell [9] carried out studies on the angle-of-attack effects of a 3-degree-of-freedom airfoil model with freeplay in the flap rotation. A vortex lattice aerodynamic model and a reduced order aerodynamic technique were used to calculate unsteady aerodynamic forces in a low subsonic region. The LCO and chaotic motion occurred over a wide range of velocities for small angles of attack, and the responses converged to a static equilibrium state as the angle of attack increased.

In this study, an efficient aeroelastic analysis method that can deal with aerodynamic nonlinearity due to transonic shock waves and structural nonlinearity due to freeplay is presented. The fictitious mass method is used to apply a modal approach to nonlinear structural models. The TSD equation is used to calculate unsteady aerodynamic forces in the transonic region. Nonlinear aeroelastic

responses are computed by the coupled time integration method in the time domain. Finally, for an all-movable wing with freeplay, the nonlinear aeroelastic responses in a transonic Mach number were compared with those in a subsonic Mach number at various freeplay angles and initial disturbances.

II. Equations of Motion and Computational Method

The equation of motion of an aeroelastic system with structural nonlinearities can be written as

$$[M]\{\ddot{u}\} + [C]\{\dot{u}\} + \{R(u)\} = \{F(t, u, \dot{u})\} \tag{1}$$

The structural nonlinear restoring force vector $\{R(u)\}$ can be written as

$$\{R(u)\} = [K]\{u\} + \{f(\alpha)\} \tag{2}$$

The restoring force vector due to structural nonlinear factors $\{f(\alpha)\}$ is given as

$$f(\alpha) = \begin{cases} K_\alpha(\alpha - s), & \alpha > s \\ 0, & -s \le \alpha \le s \\ K_\alpha(\alpha + s), & \alpha < -s \end{cases} \tag{3}$$

Generally, the aeroelastic analysis is conducted by using a mode approach method with a limited number of low frequency modes to reduce computational effort. In general the normal mode approach cannot be used directly due to stiffness variation with the displacement for air vehicle wings with freeplay. To overcome this difficulty, Karpel [10] proposed the fictitious mass method. Lee and Kim [11] describe the application of the FM method to a 3-D wing with freeplay. After the modal matrix $[\phi_b]$ is obtained from the fictitious mass model, the displacement vector can be expressed as

$$\{u(t)\} = [\phi_b]\{q(t)\} \tag{4}$$

Transformation of Eq. (1) into the modal coordinate system gives

$$[GM]\{\ddot{q}\} + [GC]\{\dot{q}\} + \{GR(u)\} = \{Q(t, q, \dot{q})\} \tag{5}$$

$\{Q\}$ can be obtained from summation of the pressure distribution on the wing surfaces, which is obtained from the TSD equation

$$\{Q\} = [\phi_b]^T \frac{1}{2}\rho U^2 \iint_S \Delta C_p \, \mathrm{d}S \tag{6}$$

ΔCp is computed from an aerodynamic analysis at each time step. The theory and application method of the TSD equation are described in detail in [6,12]. For the numerical time integration, the fifth order Runge–Kutta algorithm is used after transformation of the aeroelastic equation of motion for the generalized modal coordinate system into the second order state equation.

III. Results and Discussion

As a computational example, an all-movable control wing model with freeplay about its hinge axis is considered in the present study. The wing model has a root chord of 0.156 m, aspect ratio of 2.564, taper ratio of 0.5, and sweptback angle of 27.47 deg. The structural thickness of the wing is 2 mm and the linear stiffness K_α is 100 Nm/rad. For the wing section, 4% biconvex airfoil is used.

When the flow velocity increases to transonic, aerodynamic nonlinearities are important and they can have a pronounced influence on the aeroelastic characteristics. In this study, the aerodynamic nonlinearities induced by the shock waves in the transonic region are considered. Figure 1 shows the chordwise differential (lower surface minus upper) pressure coefficient distributions at the midspan for the Mach numbers 0.5, 0.85, 0.9, for a model with an initial angle of attack of 2 deg before the wing has been deformed by an angle of attack. The differential pressure distribution changes slightly as the Mach number increases in the subsonic region. At $M = 0.9$, a weak shock appears on the upper and lower surfaces of the control wing with a 0 deg angle of attack, whereas with an angle of attack, the lower surface shock disappears while the upper surface shock moves to the trailing edge. The shock waves located on the upper and lower wing surfaces move periodically with the oscillatory wing motion. Their motions are the predominant factor in the anomalies observed when the Mach number approaches unity.

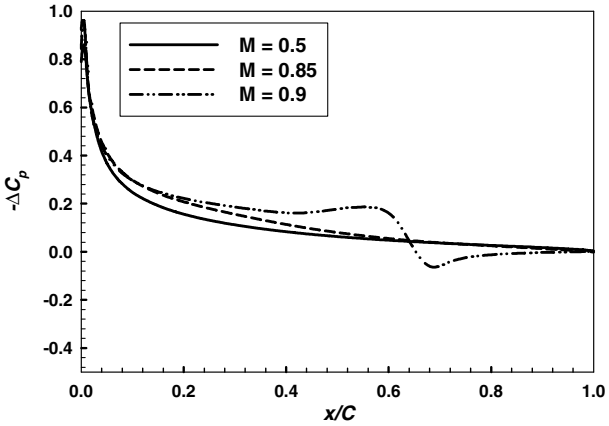

Fig. 1 Distributions of steady pressure coefficient differences at the midspan station of the undeformed wing.

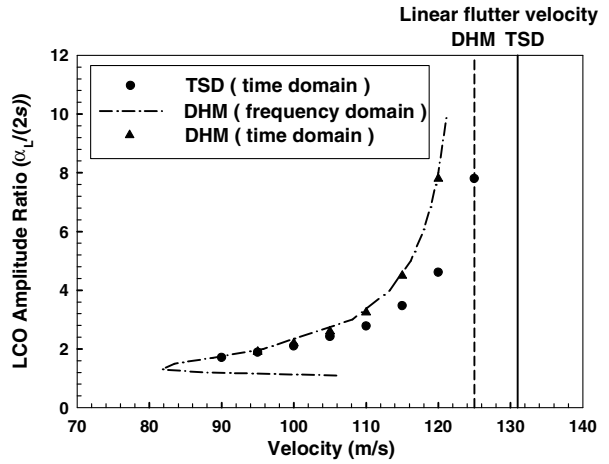

Fig. 2 LCO amplitude ratio versus velocity of the model ($M = 0.5$, initial pitch angle ratio = 4).

Figure 2 shows the LCO amplitude ratio against velocity at Mach 0.5 when the freeplay angle s is 0.1 deg and the initial pitch angle is 0.4 deg. The sea level density is used for the calculation of dynamic pressures throughout this paper. An initial condition is given by the initial pitch angle defined as the angular displacement about the hinge axis with rigid body rotation of the wing. Also, the initial pitch angle ratio is the ratio of the initial pitch angle (α_0) to the freeplay angle (s), and the LCO amplitude ratio is $\alpha_L/(2s)$, where α_L is the LCO amplitude of the pitch angle about the hinge axis. To verify the developed aeroelastic analysis system, the results using TSD aerodynamics were compared with those using the doublet hybrid method (DHM) in the subsonic region of Mach 0.5. DHM is an unsteady aerodynamic panel technique; theoretical background and its application to aeroelastic analyses in time and frequency domains are described in [5] in detail. The calculated linear flutter velocities, which are defined as the flutter velocities of the model with zero freeplay angle, are 130.9 and 125.4 m/s using the TSD aerodynamics and the DHM, respectively. It is shown in Fig. 2 that the LCOs have been found over a wide range of velocity for the wing. The calculated aeroelastic responses of the time domain TSD case are

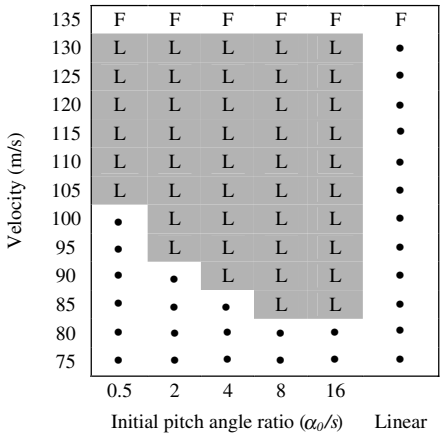

a) M=0.5

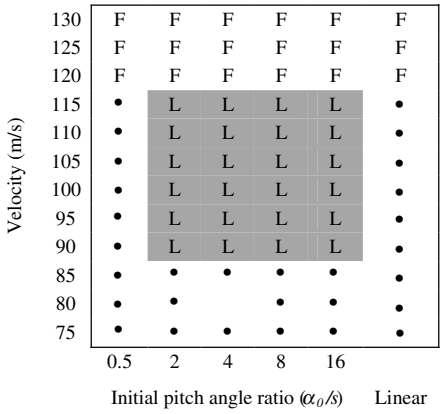

b) M=0.9

Fig. 3 Parameter maps for various initial pitch angle ratios: $s = 0.1$ deg; (F: flutter; L: LCO; ●: damped stable motion).

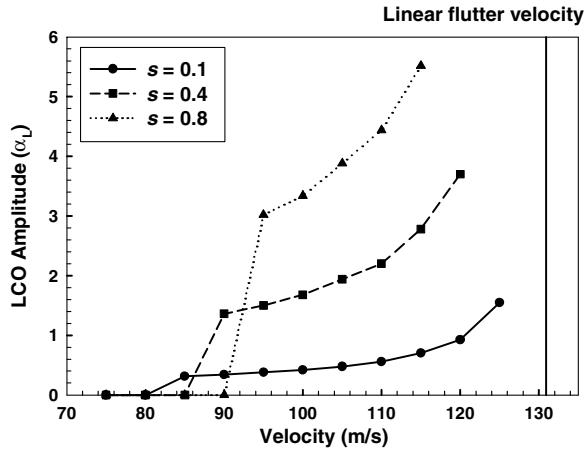

a) M=0.5

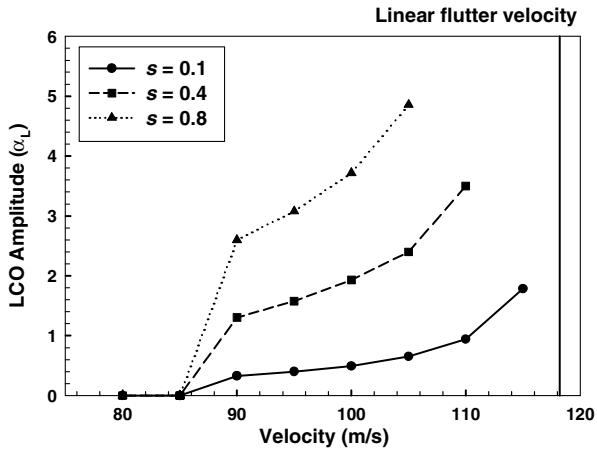

b) M=0.9

Fig. 4 LCO amplitude versus velocity of the model (initial pitch angle = 1.6 deg).

decayed out and converge to some arbitrary static equilibrium position at velocities below 90 m/s. As the airflow velocity was increased past that value, the LCO response appeared and the LCO amplitude increased exponentially and diverged at the linear flutter velocity. Both the TSD and the DHM methods estimated the onset velocities of the LCO and their amplitude trends close to each other, considering the difference in the linear flutter velocities obtained by the two methods.

Figure 3 shows the parameter maps for various initial pitch angle ratios at Mach 0.5 and 0.9. The analyses were carried out at 0.05, 0.2, 0.4, 0.8, and 1.6 deg initial pitch angles when the freeplay angle was fixed at 0.1 deg. The nonlinear flutter velocity almost agreed with the linear flutter velocity for both Mach numbers and was steady regardless of the initial pitch angle ratio variation. The LCOs were also generated over a wide range of velocity below the nonlinear flutter velocity. In the case of Mach 0.5, the onset velocity of the LCO decreased as the initial pitch angle ratio increased. Thus, the velocity range in which the LCO could occur was widened. For Mach 0.9, however, when the initial pitch angle ratio was less than 1.0, that is, the initial pitch angle was in the range of freeplay, the LCO did not occur. Over the initial pitch angle ratio of 1.0, the range of the LCO onset velocity was radically increased and was then kept steady as the initial pitch angle ratio increased. Compared with the case of Mach 0.5, it was found that the LCO onset velocity range was narrower and was affected less by the initial disturbance at Mach 0.9.

The LCO amplitude versus velocities with the freeplay angles for Mach 0.5 and 0.9 are shown in Fig. 4. The analyses were accomplished at freeplay angles of 0.1, 0.4, and 0.8 deg with the initial pitch angle fixed at 1.6 deg. As the size of freeplay increased, the LCO amplitude increased and the nonlinear flutter velocity decreased below the linear flutter velocity at both Mach 0.5 and 0.9. The LCOs were also found in a wide range of velocity below the nonlinear flutter velocity. In the case of Mach 0.5, the LCO onset velocity increased with the size of freeplay. Thus, the velocity range for LCO occurrence decreased. At Mach 0.9, however, the LCO onset velocity was independent of the size of freeplay.

IV. Conclusions

In this study an efficient aeroelastic analysis method was developed to deal with the aerodynamic nonlinearity caused by shock waves in the transonic region and the structural nonlinearity caused by freeplay. This method was then applied to a 3-D all-movable control wing to investigate its nonlinear aeroelastic responses. The effects of the initial disturbance decreased in the transonic region compared with those in the subsonic region. As the size of the freeplay angle increased, the LCO amplitude increased and the nonlinear flutter velocity decreased in both the subsonic and transonic regions, which indicates degradation of the aeroelastic characteristics.

Acknowledgments

The authors are gratefully acknowledging the support by the Agency for Defense Development and the FVRC (Flight Vehicle Research Center), Seoul National University.

References

[1] Lee, B. H. K., and Tron, A., "Effects of Structural Nonlinearities on Flutter Characteristics of the CF-18 Aircraft," *Journal of Aircraft*, Vol. 26, No. 8, 1989, pp. 781–786.

[2] JSSG-2006, "Department of Defense Joint Service Guide (Aircraft Structures)," 30 Oct. 1998, pp. 341–343.
[3] Laurenson, R. M., and Trn, R. M., "Flutter Analysis of Missile Control Surfaces Containing Structural Nonlinearities," *AIAA Journal*, Vol. 18, No. 10, 1980, pp. 1245–1251.
[4] Kim, S. H., and Lee, I., "Aeroelastic Analysis of a Flexible Airfoil with a Freeplay Nonlinearity," *Journal of Sound and Vibration*, Vol. 193, No. 193, 1996, pp. 823–846.
[5] Bae, J. S., Yang, S. M., and Lee, I., "Linear and Nonlinear Aeroelastic Analysis of a Fighter-Type Wing with Control Surface," *Journal of Aircraft*, Vol. 39, No. 4, 2002, pp. 697–708.
[6] Kim, D. H., and Lee, I., "Transonic and Low-Supersonic Aerodynamic Analysis of a Wing with Underpylon/Store," *Journal of Aircraft*, Vol. 37, No. 1, 2000, pp. 189–192.
[7] Kousen, K. A., and Bendiksen, O. O., "Nonlinear Aspects of the Transonic Aeroelastic Stability Problem," AIAA Paper 88-2306, April 1988.
[8] Kousen, K. A., and Bendiksen, O. O., "Limit Cycle Phenomena in Computational Transonic Aeroelasticity," *Journal of Aircraft*, Vol. 31, No. 6, 1994, pp. 1257–1263.
[9] Kholodar, D. B., and Dowell, E. H., "Behavior of Airfoil with Control Surface Freeplay for Nonzero Angle of Attack," *AIAA Journal*, Vol. 37, No. 5, 1999, pp. 651–653.
[10] Karpel, M., and Wieseman, C. D., "Modal Coordinates for Aeroelastic Analysis with Large Local Structural Variation," *Journal of Aircraft*, Vol. 31, No. 2, 1994, pp. 396–400.
[11] Lee, I., and Kim, S. H., "Aeroelastic Analysis of a Flexible Control Surface with Structural Nonlinearity," *Journal of Aircraft*, Vol. 32, No. 4, 1995, pp. 868–874.
[12] Yoo, J. H., Kim, D. H., and Lee, I., "Angle-of-Attack Effect on the Transonic/Supersonic Aeroelasticity of Wing-Box Model," *Journal of Aircraft*, Vol. 39, No. 5, 2002, pp. 906–908.

C. Pierre
Associate Editor